Supplementary Information for

Three-dimensional atomic insights into the metal-oxide interface in Zr-ZrO_2 nanoparticles

Yao Zhang[1,5], Zezhou Li[1,5], Xing Tong[2,5], Zhiheng Xie[1], Siwei Huang[1], Yue-E Zhang[2,3], Hai-Bo Ke[2]*, Wei-Hua Wang[2,4], Jihan Zhou[1]*

[1]*Beijing National Laboratory for Molecular Sciences, Center for Integrated Spectroscopy, College of Chemistry and Molecular Engineering, Peking University; Beijing, 100871, China.*
[2]*Songshan Lake Materials Laboratory, Dongguan 523808, China.*
[3]*College of Physics, Liaoning University, Shenyang 110036, China.*
[4]*Institute of Physics, Chinese Academy of Sciences, Beijing 100190, China.*
[5]*These authors contributed equally to this work.*
**Correspondence and requests for materials should be addressed to H.-B. K. (email: kehaibo@sslab.org.cn) and J. Z. (email: jhzhou@pku.edu.cn)*

Supplementary Table 1 Tomography and reconstruction overview.

	Zr1	Zr2	Zr3
Data Collection and Processing			
Voltage (kV)	300	300	300
Convergence semi-angle (mrad)	21.4	21.4	21.4
Detector inner angle (mrad)	39.4	31.5	31.5
Detector outer angle (mrad)	200	190.6	190.6
Pixel size (Å)	0.343	0.343	0.343
Scanning current (pA)	15	15	15
Number of projections	50	59	57
Tilt range (°)	-75 76	-76 77	-75 75.5
Electron dose (10^5 e $Å^{-2}$)	4.8	3.4	2.9
Reconstruction			
Algorithm	RESIRE		
Oversampling ratio	4	4	4
Number of iterations	200	200	200
Reconstruction error (%)	0.1069	0.0728	0.0990
Number of atoms	15392	22382	13482

Supplementary Table 2 Summary of multi-slice simulation parameters.

Slice thickness	2 Å
Debye-Waller factor	0.3 $Å^2$
Acceleration voltage	300 kV
Convergence angle	30 mrad
Detector collection range	[39.4 – 200] mrad
FWHM of the point spread function	80 pm
Pixel size of simulated image	0.3434 Å
Pixel size to sample atomic potential	0.1 Å
Frozen phonons	4
Screen current*	30 pA

*The screen current is only applied for Supplementary Figs. 7d, 8b, and related analysis.

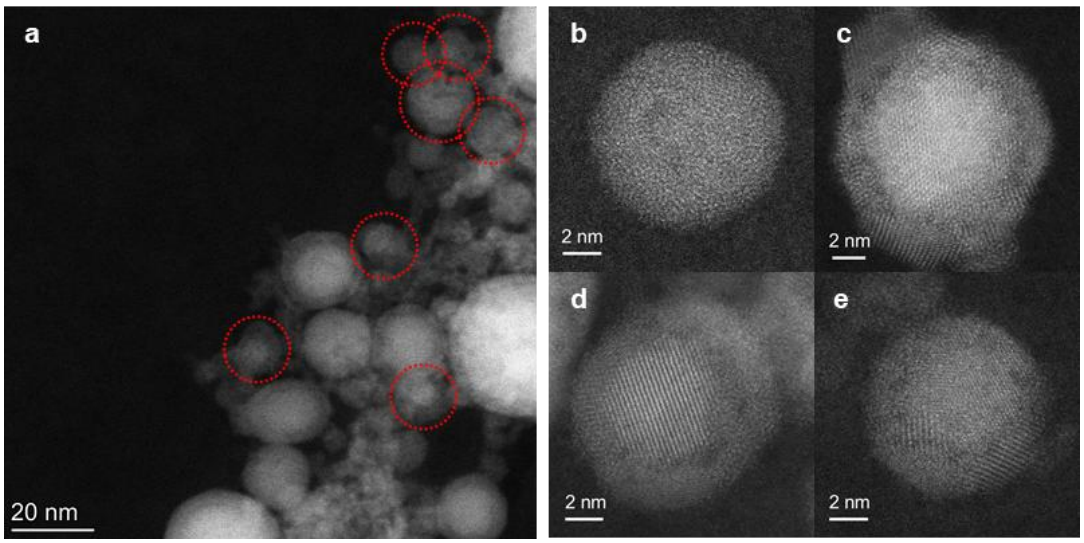

Supplementary Figure 1 ADF-STEM images show the Zr-ZrO_2 NPs with an oxidized shell and a metal core. a, Overview of the oxidized Zr NPs. Some particles similar to Zr1 NP are marked by the red dashed circles. **b-e**, Representative high-resolution images show the different morphologies of Zr-ZrO_2 NPs with a diameter of around 10 nm. Some of the nanoparticles are completely oxidized (**b, d**), and some have a metal core and an oxide shell (**c, e**).

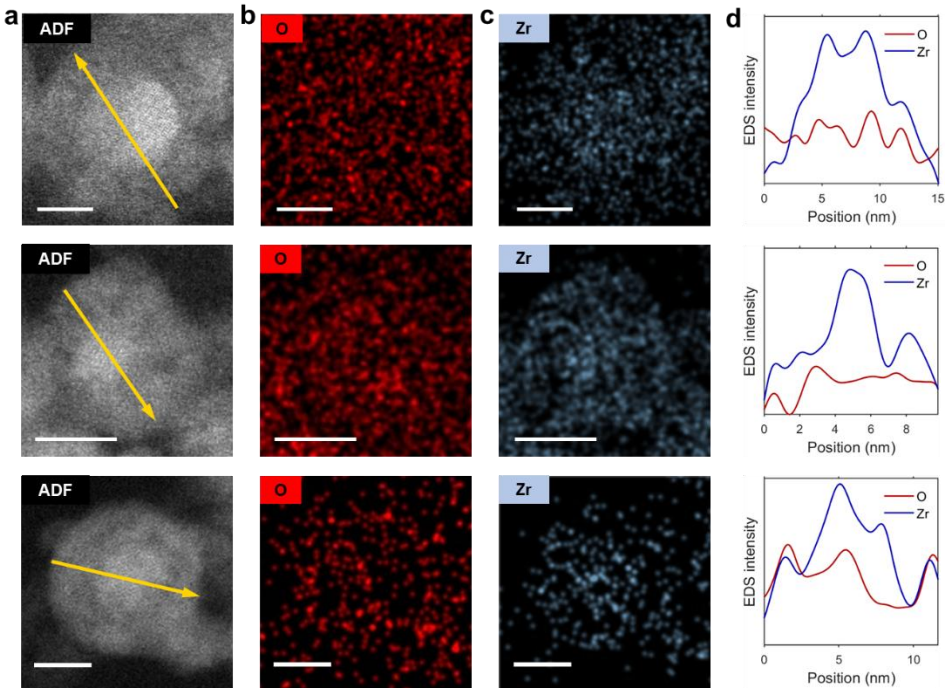

Supplementary Figure 2 EDS mapping and line profiles show the elements distribution of Zr-ZrO_2 NPs. The ADF-STEM images of different Zr-ZrO_2 NPs (**a**) and their corresponding O (**b**; in red), Zr (**c**; in blue) EDS maps. The line profiles (**d**) along the yellow arrows in (**a**) show high Zr signals and low O signals at the center of the NP, with O in red and Zr in blue. Source data for Supplementary Fig. 2d are provided as a Source Data file.

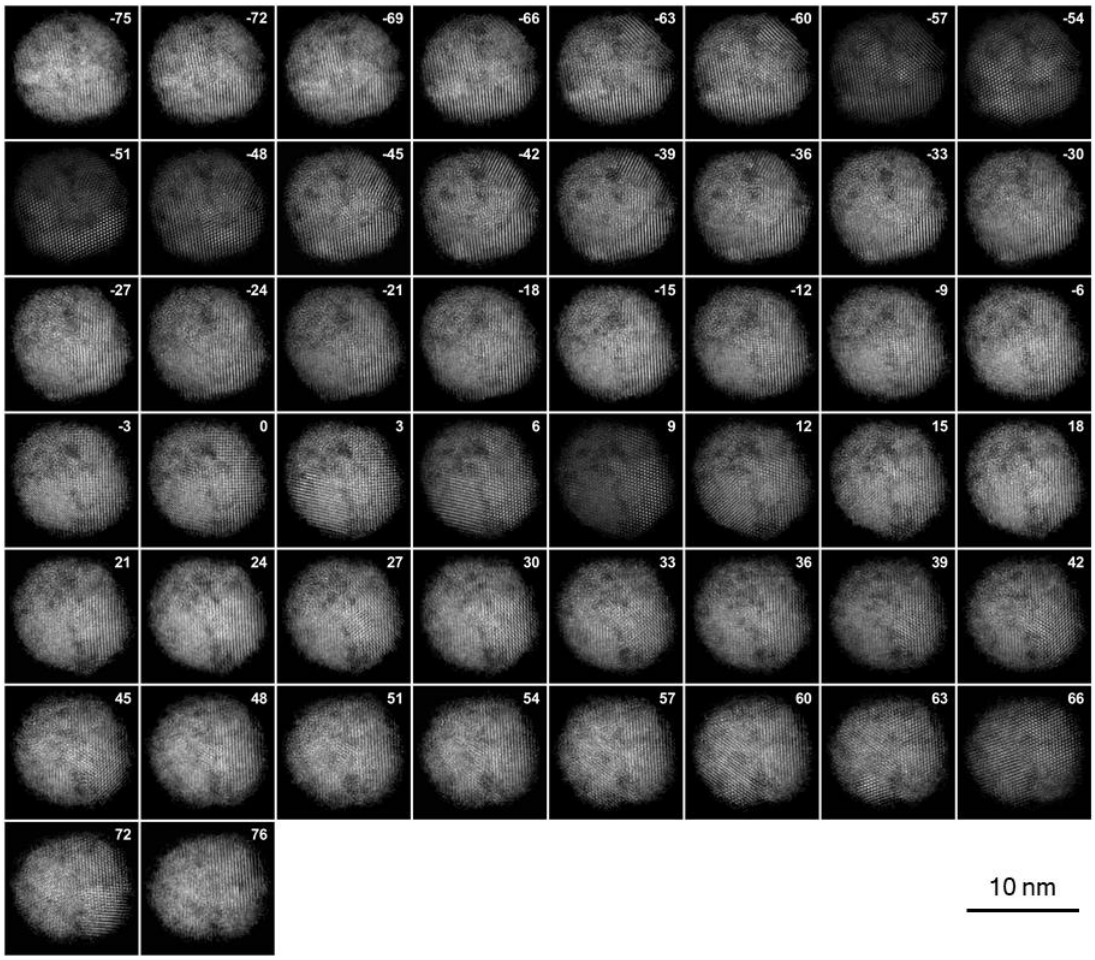

Supplementary Figure 3 Tomography tilt series of the Zr1 NP. 50 ADF-STEM images with a tilt range from -75.0° to +76.0°.

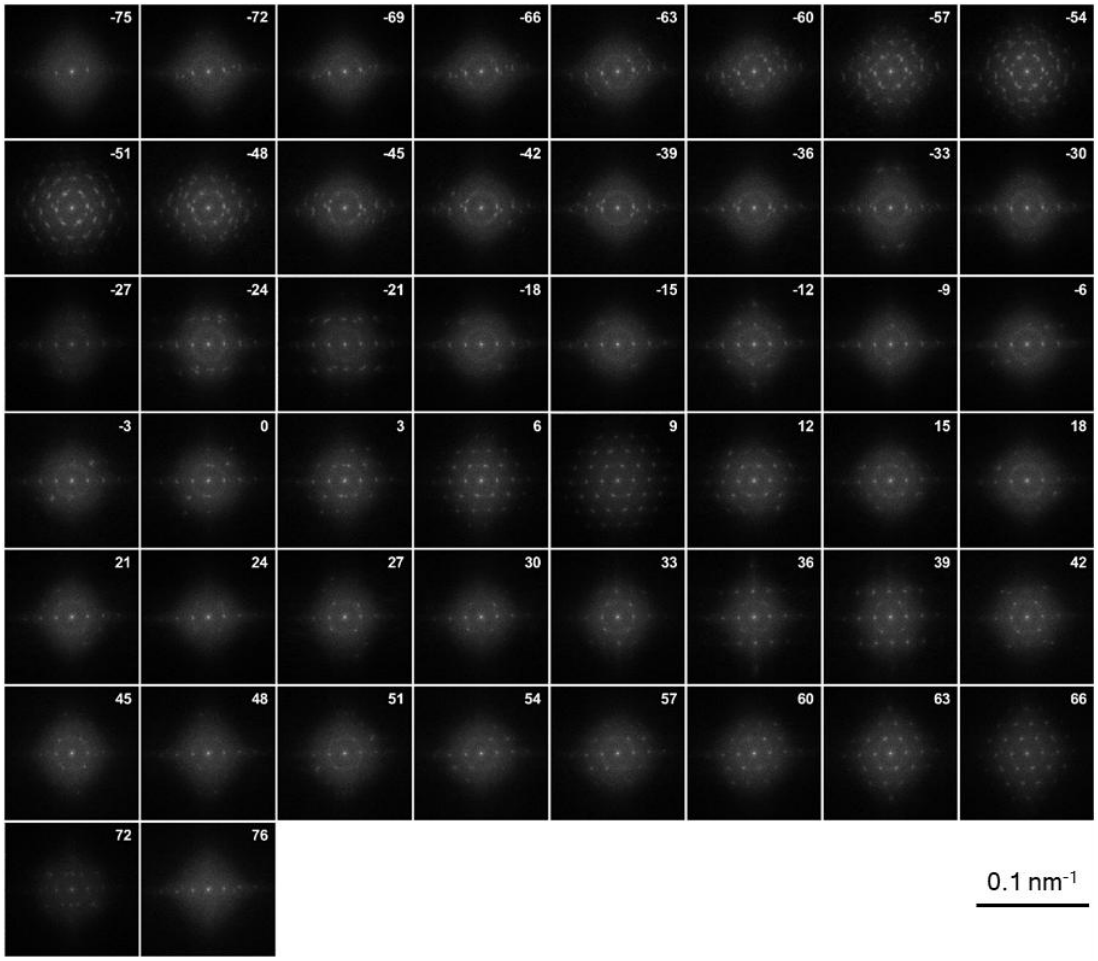

Supplementary Figure 4 FFT of the tomography tilt series of the Zr1 NP. FFT of the 50 ADF-STEM images with a tilt range from -75.0° to +76.0°.

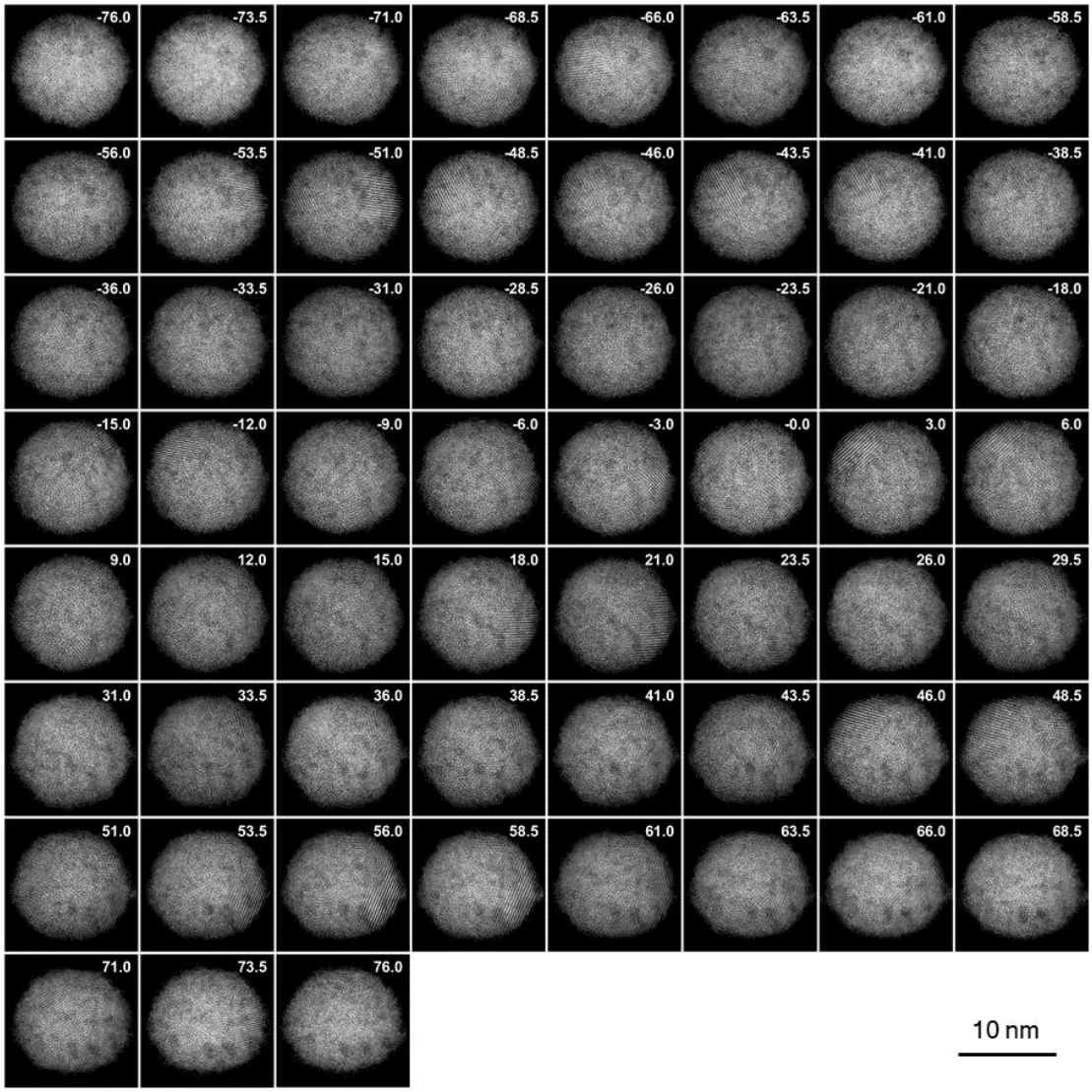

Supplementary Figure 5 Tomography tilt series of the Zr2 NP. 59 ADF-STEM images with a tilt range from -76.0° to +77.0°.

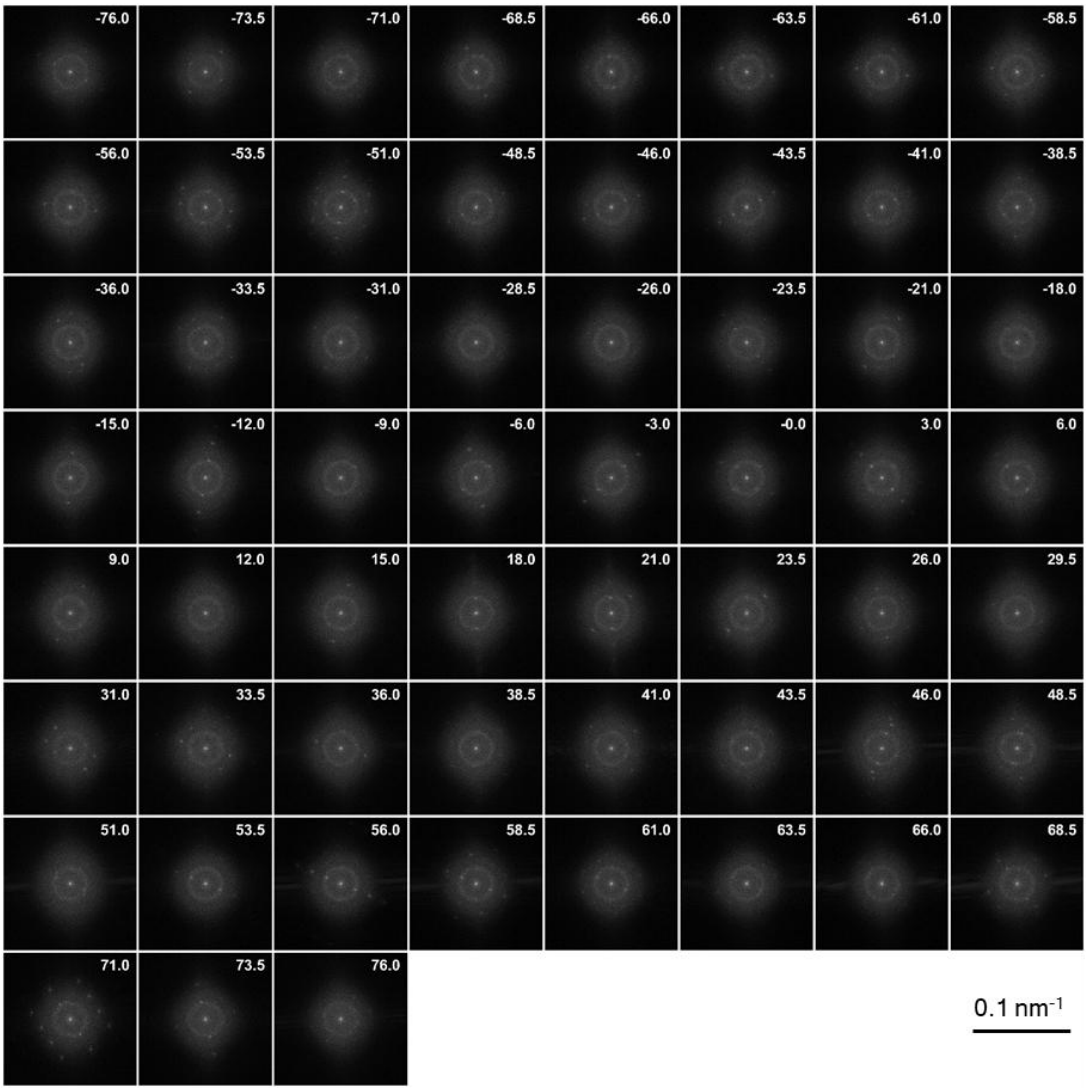

Supplementary Figure 6 FFT of the tomography tilt series of the Zr2 NP. FFT of the 59 ADF-STEM images with a tilt range from -76.0° to +77.0°.

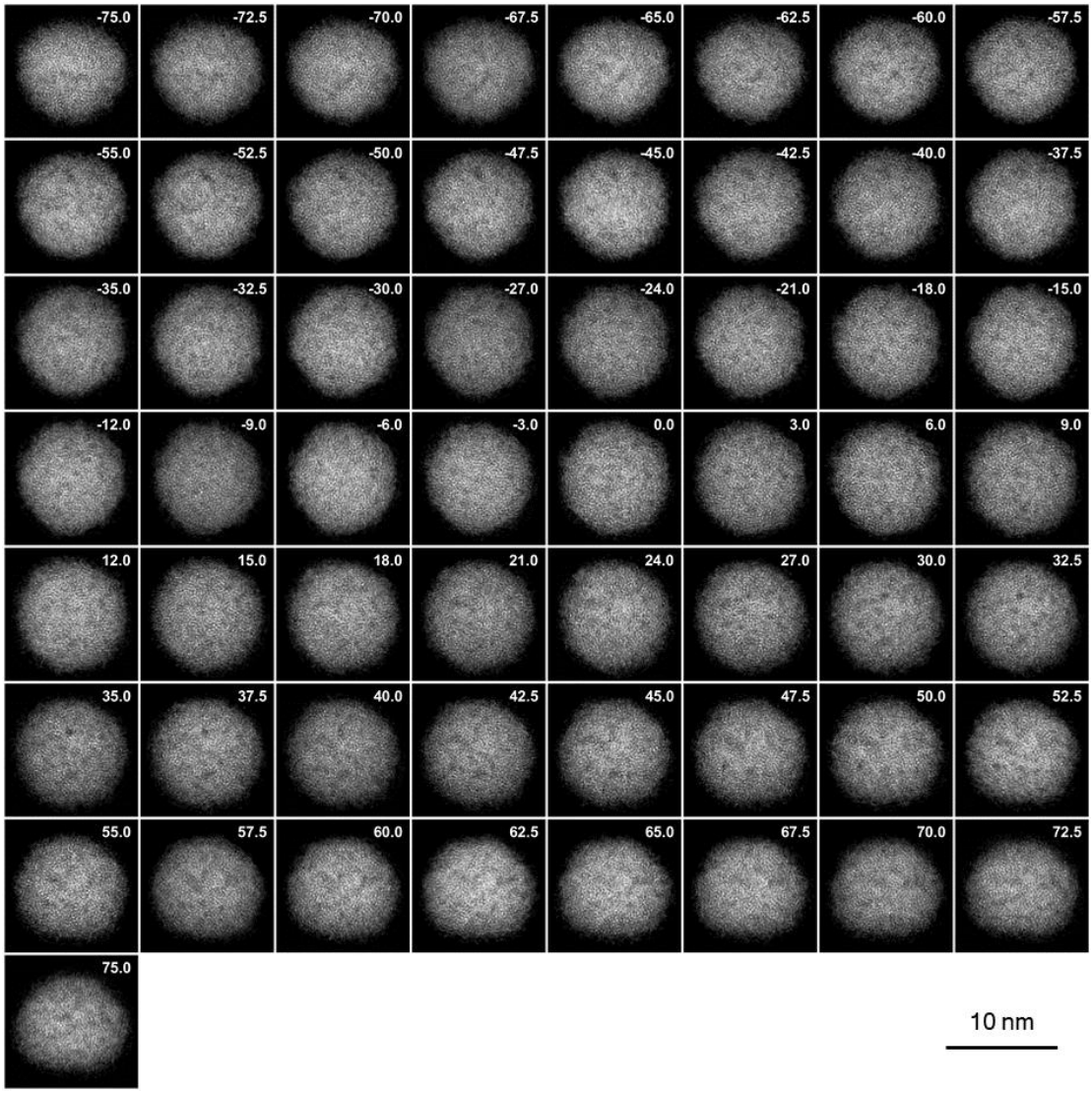

Supplementary Figure 7 Tomography tilt series of the Zr3 NP. 57 ADF-STEM images with a tilt range from -75.0° to +75.5°.

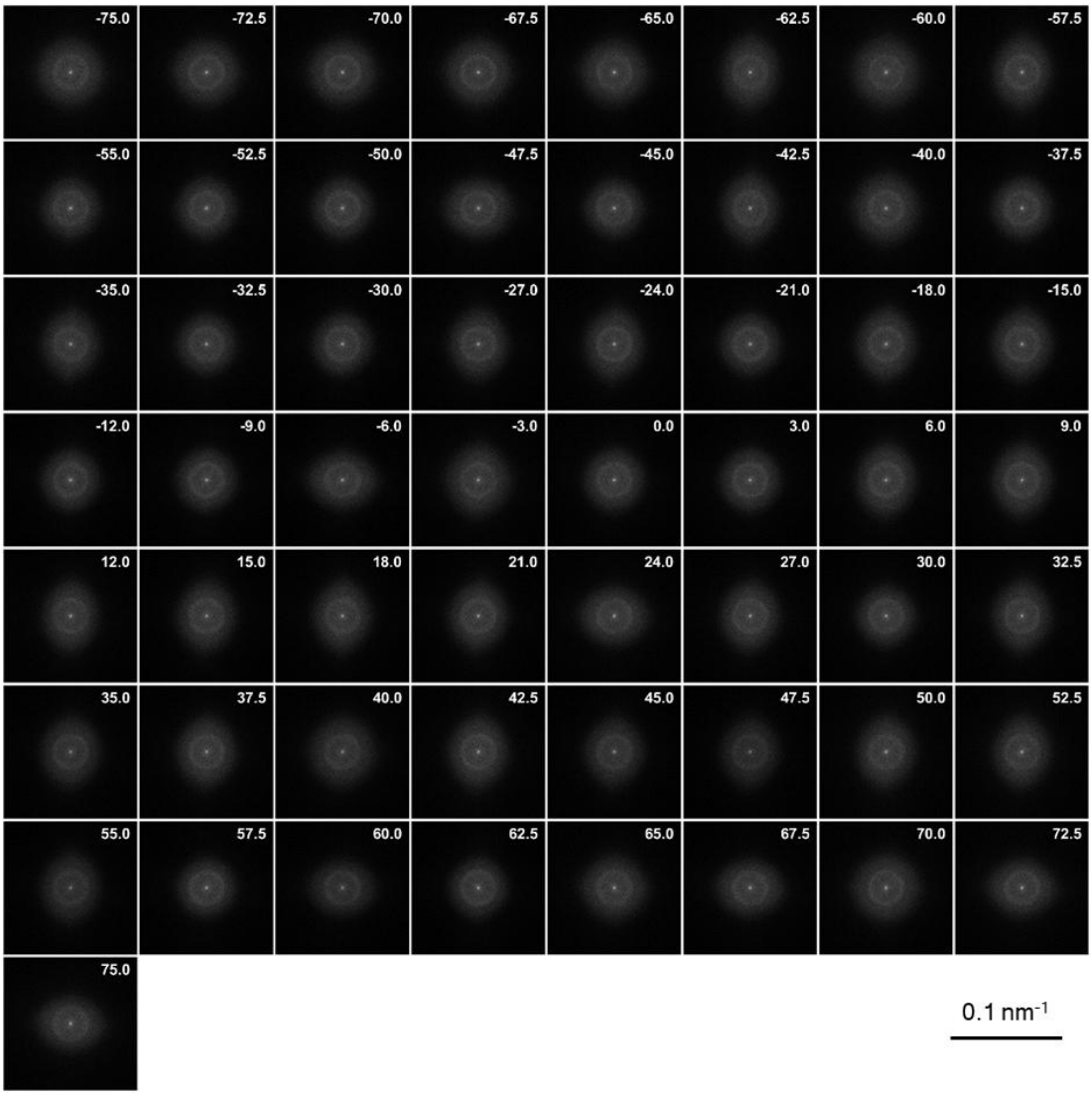

Supplementary Figure 8 FFT of the tomography tilt series of the Zr3 NP. FFT of the 57 ADF-STEM images with a tilt range from -75.0° to +75.5°.

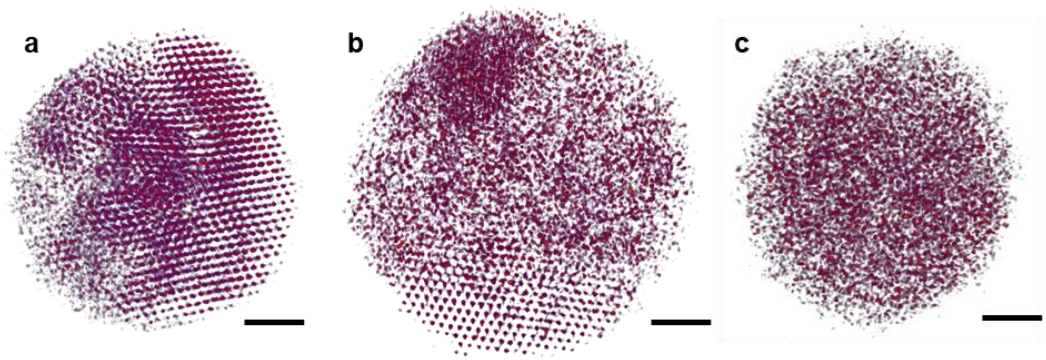

Supplementary Figure 9 Volume rendering of raw reconstructions. Volume rendering of raw reconstructions of Zr1 (**a**), Zr2 (**b**), and Zr3 (**c**) NPs. Scale bars, 2 nm.

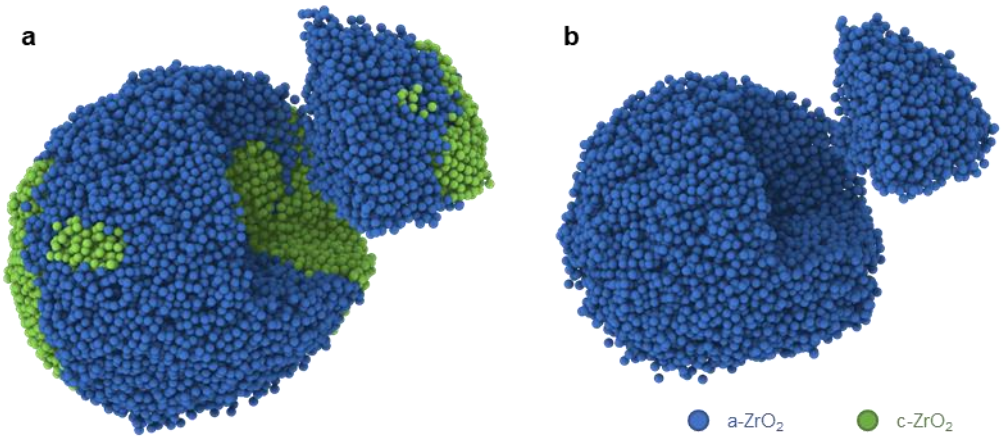

Supplementary Figure 10 Atomic model for Zr2 and Zr3 NPs. a, Atomic model for Zr2 NP, with crystalline oxide grains (c-ZrO_2; in green) and a large amorphous oxide phase (a-ZrO_2; in blue). **b**, Atomic model for Zr3 NP, which contains a-ZrO_2 only.

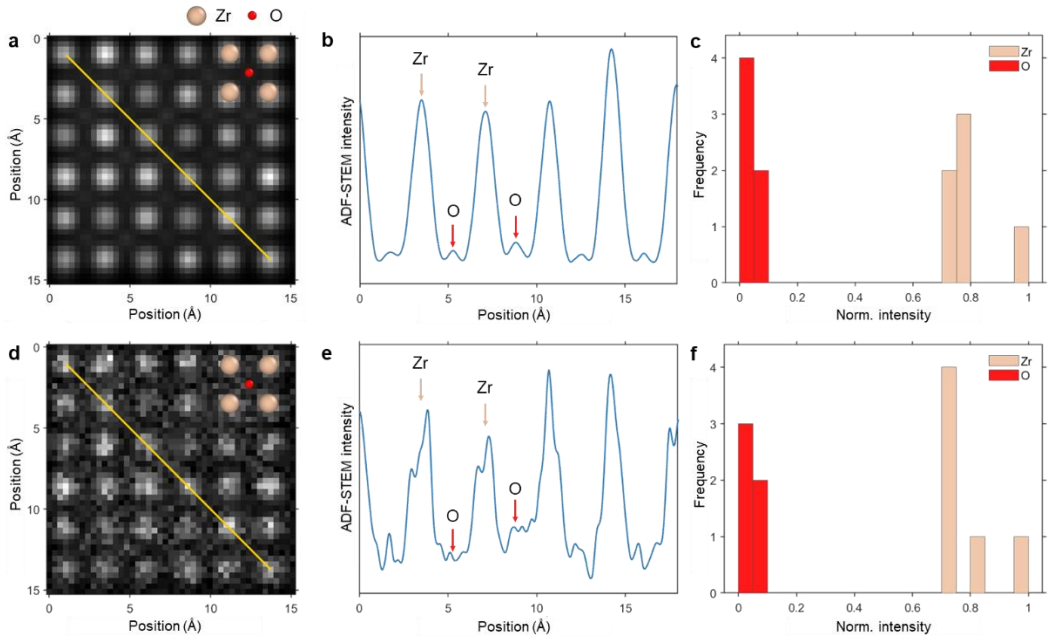

Supplementary Figure 11 Multi-slice simulation of the ADF-STEM images of ZrO_2. a-c, Noise-free ADF-STEM image (**a**) of the 8-nm-thick c-ZrO_2 slab by multi-slice simulation along the [100] zone axis. The line profile (**b**) along the yellow line in panel **a** shows the intensity of Zr columns and O columns. The ivory arrows and red arrows show the position of Zr atoms and O atoms, respectively. (**c**) The intensity histograms of all Zr columns and O columns. The oxygen column intensity is typically 1/10 of the zirconium column intensity. **d-f**, Noise-added ADF-STEM image (**d**) of the 8-nm-thick c-ZrO_2 slab by multi-slice simulation along the [100] zone axis. The electron dose is determined according to the experimental conditions. The line profile (**e**) along the yellow line in panel **d** shows the intensity of Zr columns and O columns. The ivory arrows and red arrows show the position of Zr atoms and O atoms, respectively. The oxygen column contrast is much lower. (**f**) The intensity histograms of all Zr columns and O columns. In panel **a** & **d**, the Zr atoms and O atoms are colored in ivory and red, respectively. The parameters for the multi-slice simulation are listed in Supplementary Table 2. These simulation results show contrast of oxygen atoms is too light to be detected in 2D. Source data for Supplementary Fig. 11b,e are provided as a Source Data file.

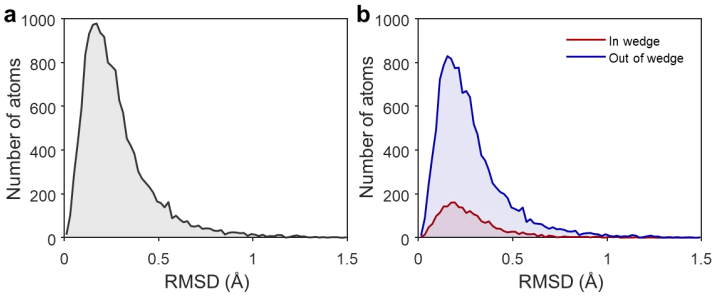

Supplementary Figure 12 Comparison of experimental model with 3D multi-slice simulated model of Zr1 nanoparticles. a, Histogram of the root-mean-square deviation (RMSD) between the experimental 3D atomic model and the new 3D atomic model traced from simulated reconstructions. By comparing experimental model with multi-slice one, we estimated that 97.2% of atoms were identified correctly with a 3D precision of 28 pm. **b**, Histogram of the RMSD of atoms in missing wedge direction, and atoms out of missing wedge direction, respectively. Source data for Supplementary Fig. 12 are provided as a Source Data file.

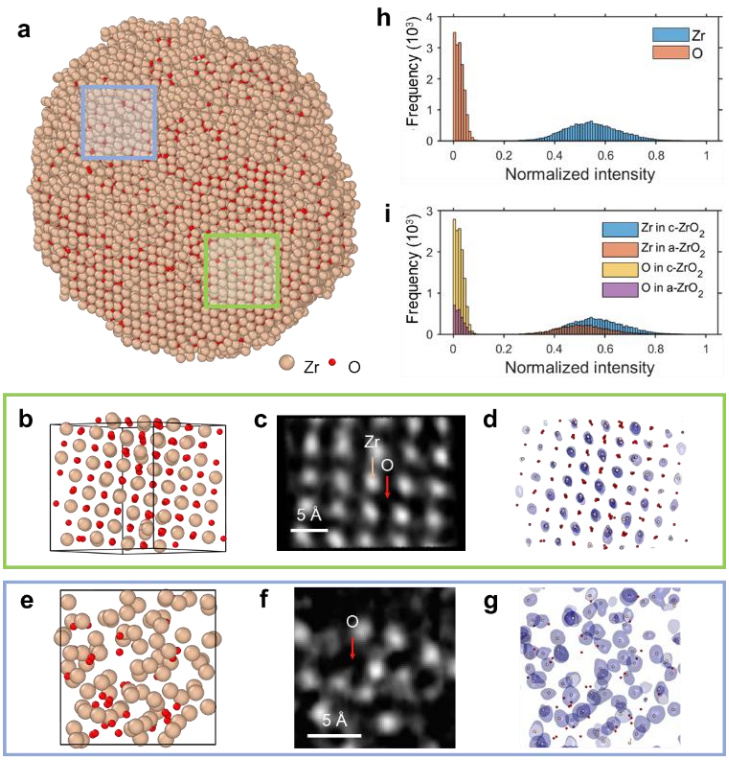

Supplementary Figure 13 The 3D reconstruction obtained from the generated tilt series of the oxygen-filling atomic model. a, The atomic model for multi-slice simulation built by filling oxygen atoms into the Zr1 experimental model (Methods). The simulated tilt series show in Supplementary Fig. 11. **b-d**, A representative atomic cut-out from c-ZrO_2 region highlighted by the green square box in (**a**), viewing from the [100] zone axis of cubic ZrO_2. **b**, The atomic model of this representative c-ZrO_2 cut-out. The edge length of this cut-out is 15 Å. **c**, A 4-Å-thick slice from the corresponding 3D reconstructed volume. The ivory and red arrows show the positions of Zr and O atoms, respectively. **d**, 3D surface renderings of all the atoms in the specified cut-out, clearly indicating the intensity in oxygen positions are way too weak comparing to the Zr sites. The atom positions are displayed in this panel for a better comparison. **e-g**, A representative atomic cut-out from a-ZrO_2 region highlighted by the blue square box in (**a**). **e**, The atomic model of this representative a-ZrO_2 cut-out. The edge length of this cut-out is 15 Å. **f**, A 2.5-Å-thick slice from the corresponding 3D reconstructed volume. The red arrow shows the position of an O atom. **g**, 3D surface renderings of all the atoms in the specified cut-out, clearly indicating the intensity in oxygen positions are way too weak comparing to the Zr sites. The atom positions are displayed in this panel for a better comparison. **h**, The intensity distribution of Zr and O atoms in the raw reconstructed volume. **i**, The intensity distribution of Zr and O atoms in a-ZrO_2 and c-ZrO_2 regions separately. In panel **a**, **b**, **d**, **e**, **g**, the Zr atoms and O atoms are colored in ivory and red, respectively. The parameters for the multi-slice simulation are listed in Supplementary Table 2. These simulation results show contrast of oxygen atoms is too light to be traced in 3D.

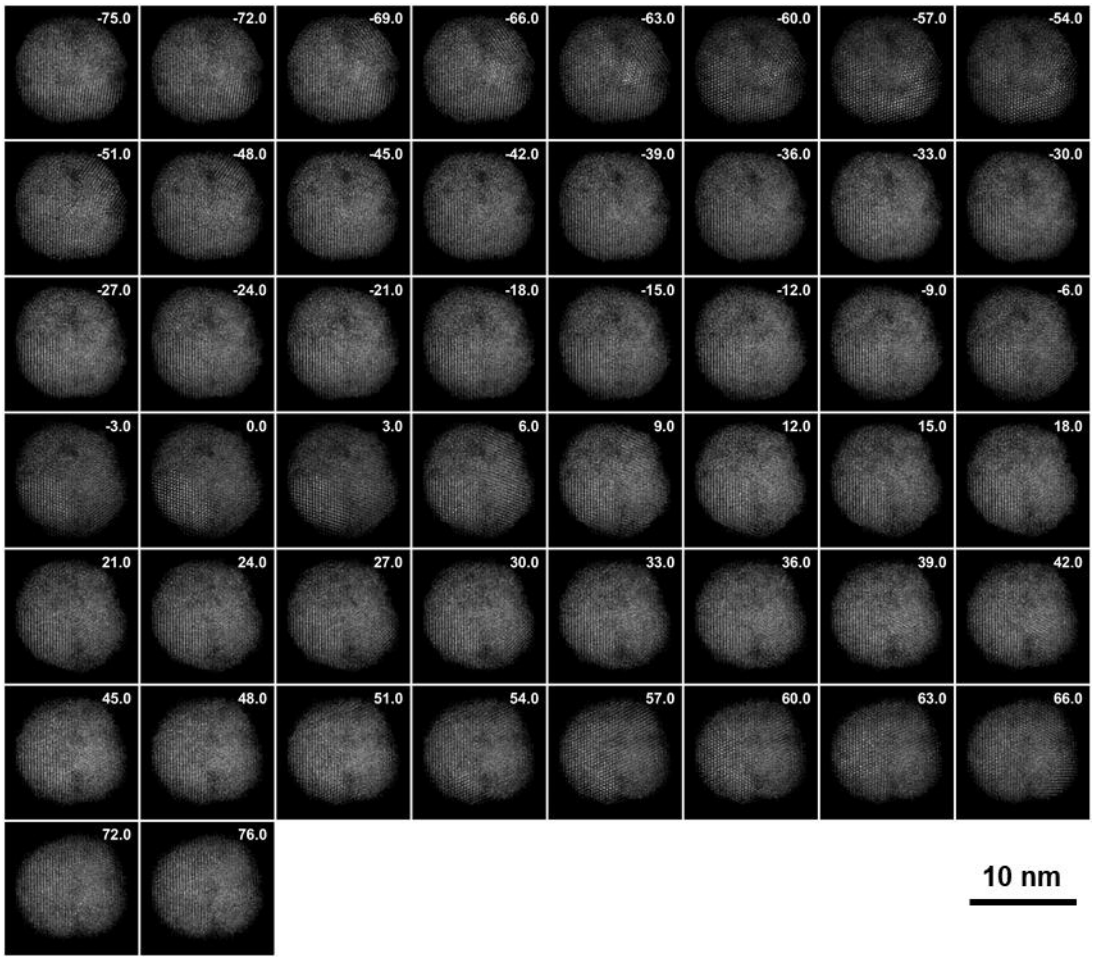

Supplementary Figure 14 The simulated tilt series. The simulated tilt series with same number of projections to the experimental one in Supplementary Fig. 3, generated by the multi-slice simulation.

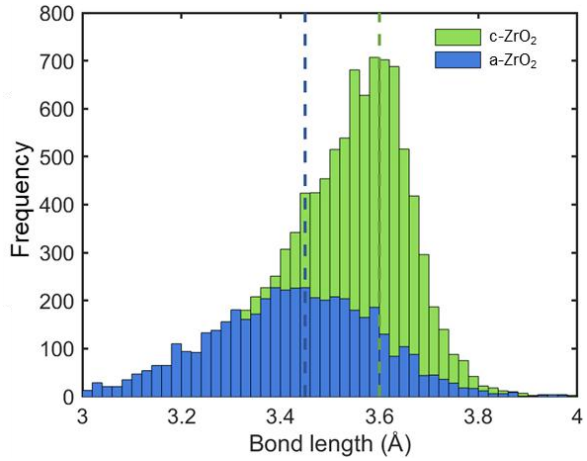

Supplementary Figure 15 Bond length distribution of Zr1 NP, with c-ZrO_2 in green and a-ZrO_2 in blue. The histogram shows the distribution of bond length in c-ZrO_2 and a-ZrO_2. The dashed lines show the most populated bond length in c-ZrO_2 (3.6 Å; the green line) and a-ZrO_2 (3.45 Å; the blue line).

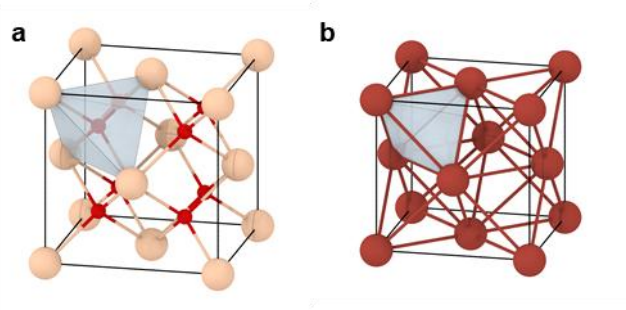

Supplementary Figure 16 The volume difference of the tetrahedral site in pure FCC Zr and c-ZrO_2. a, The tetrahedral site in c-ZrO_2, which accommodates one oxygen atom. The atoms in ivory are oxide Zr atoms, and the atoms in red are O atoms. **b**, The tetrahedral site in FCC Zr. The atoms in deep red are metal Zr atoms. Both in (**a**) and (**b**), the tetrahedron is displayed with surface rendering in light blue.

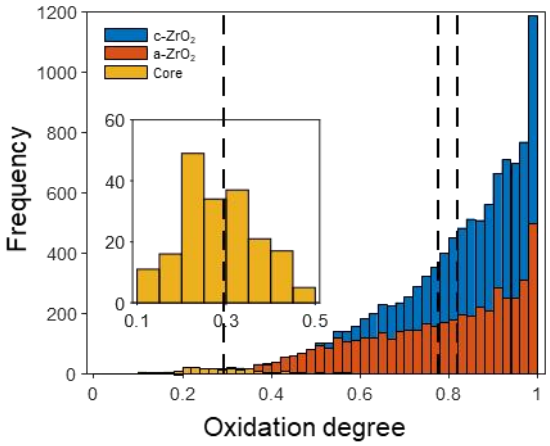

Supplementary Figure 17 The distribution of the degree of oxidation. The histogram shows the distribution of the degree of oxidation in c-ZrO_2, a-ZrO_2 and metal core. The dashed lines are the mean values of the degree of oxidation for c-ZrO_2 (0.82), a-ZrO_2 (0.78) and metal core (0.29) from right to left. The inset figure shows the magnified histogram of metal core.

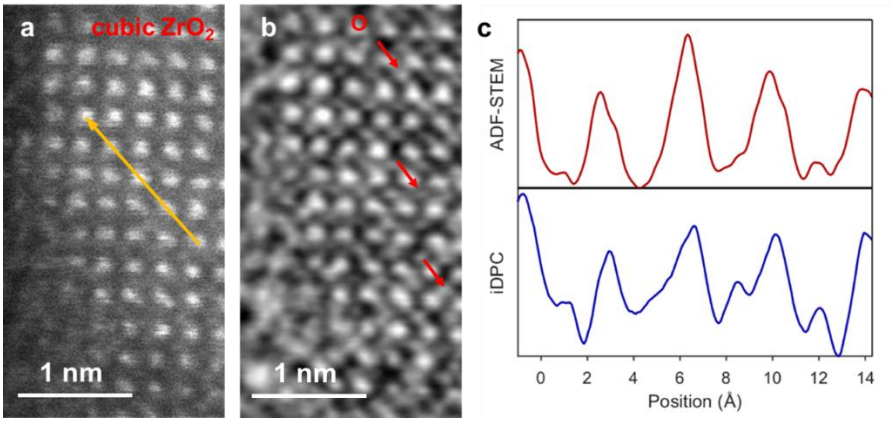

Supplementary Figure 18 Partial oxidation observed in Zr nanoparticle. The ADF-STEM image (**a**) and the corresponding iDPC (**b**) image of the cubic ZrO_2 region in the nanoparticle, viewing along [100] zone axis. The red arrows mark the positions of oxygen atomic columns in the iDPC image. **c**, The line profile of ADF-STEM (up panel of **c**) and iDPC (down panel of **c**) images along the yellow arrow in panel **a**. The difference of oxygen intensities shows the non-uniform filling of oxygen atoms due to the partial oxidation of Zr NP. Source data for Supplementary Fig. 18 are provided as a Source Data file.

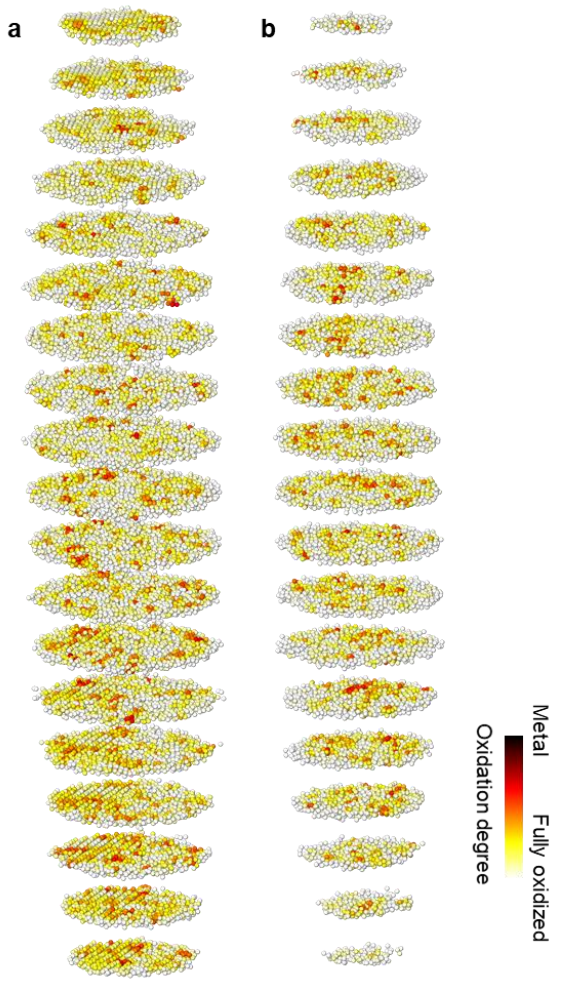

Supplementary Figure 19 Oxidation degree of Zr2 and Zr3 nanoparticles. a, Atoms of the Zr2 NP colored according to the degree of oxidation, divided into slices with a thickness of 5.3 Å. **b**, Atoms of the Zr3 NP colored according to the degree of oxidation, divided into slices with a thickness of 5.3 Å. The Zr2 and Zr3 NPs are almost completely oxidized and have high degrees of oxidation comparing to Zr1 NP.

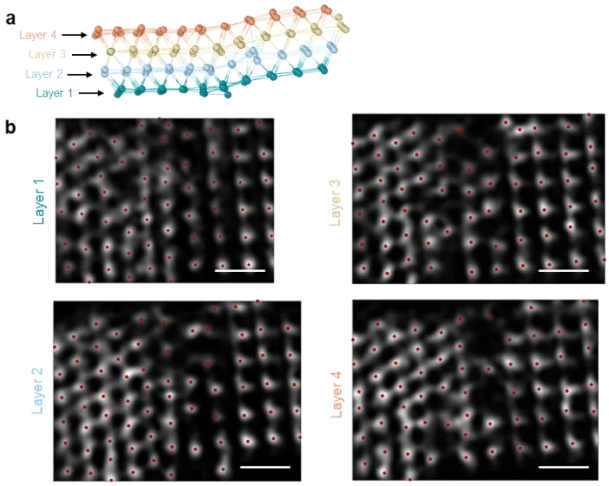

Supplementary Figure 20 The raw reconstructed intensity of the semi-coherent metal/c-ZrO_2 interface. a, The atomic model of the interface, which is the same as the one in Fig. 3e. The layers are marked by different colors. **b**, The colored layers of the sliced intensity correspond to the layers in panel **a**. The red dots highlight the positions of Zr atoms. Scale bars, 2 nm.

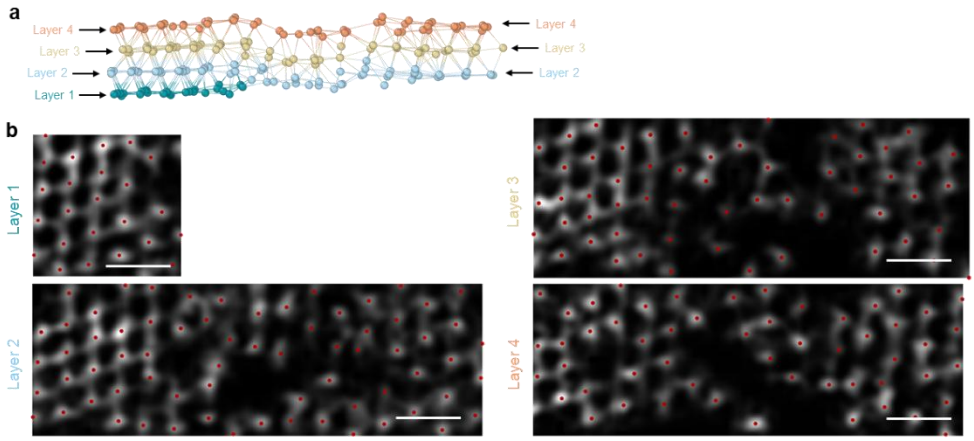

Supplementary Figure 21 The raw reconstructed intensity of the incoherent metal/c-ZrO_2 interface. a, The atomic model of the interface, which is the same as the one in Fig. 3k. The layers are marked by different colors. **b**, The colored layers of the sliced intensity correspond to the layers in panel **a**. The red dots highlight the positions of Zr atoms. Scale bars, 2 nm.

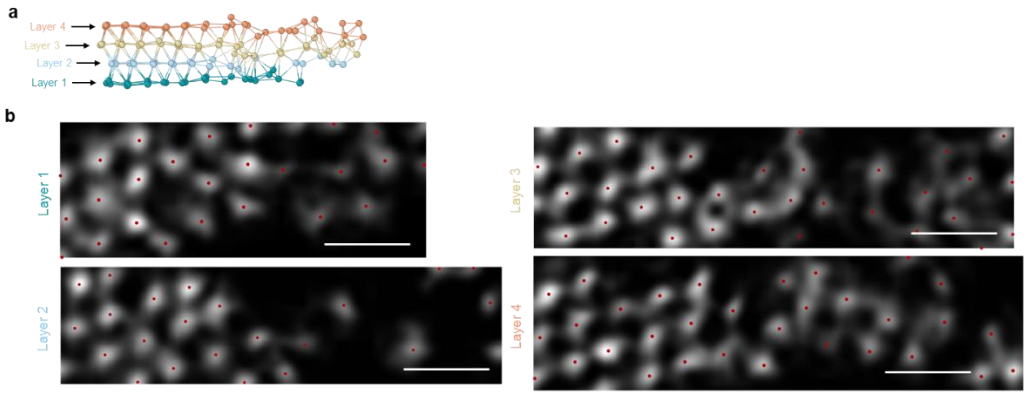

Supplementary Fig. 22 The raw reconstructed intensity of the incoherent metal/a-ZrO_2 interface. **a**, The atomic model of the interface, which is the same as the one in Fig. 3l. The layers are marked by different colors. **b**, The colored layers of the sliced intensity correspond to the layers in panel **a**. The red dots highlight the positions of Zr atoms. Scale bar, 2 nm.

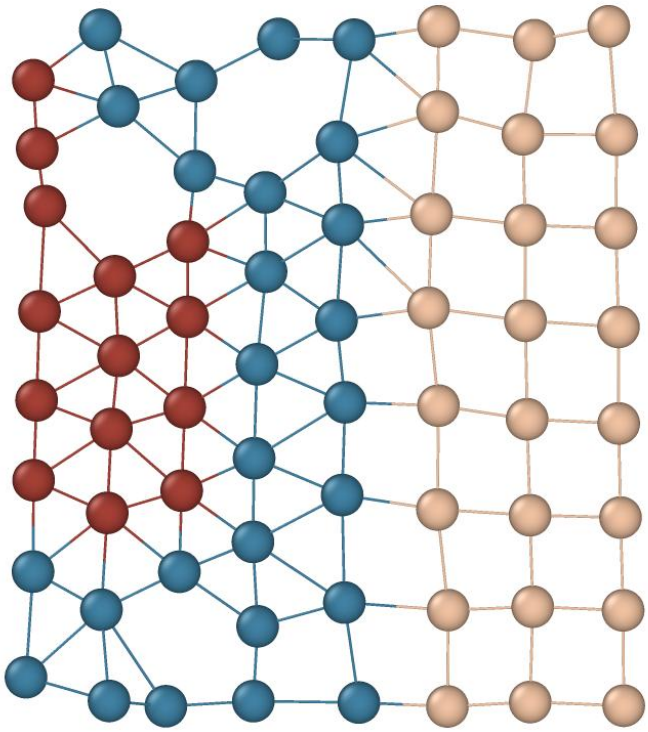

Supplementary Figure 23 The surroundings of the plane in Fig. 3g, with the dislocations and vacancies caused by semi-coherent interface. The metal atoms, interfacial atoms and oxide atoms are colored in deep red, blue and ivory, respectively.

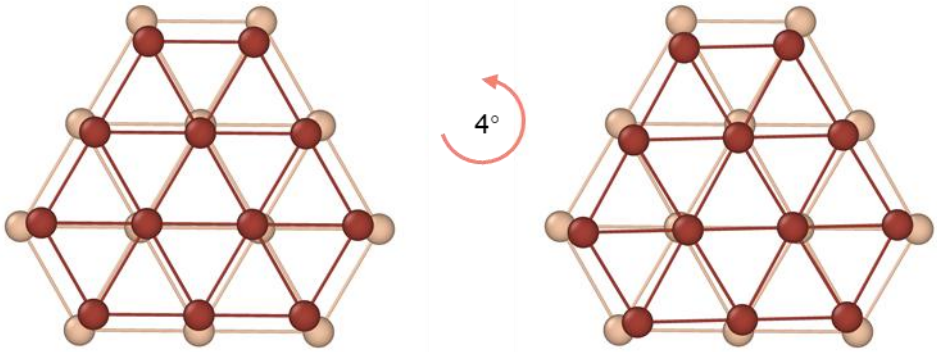

Supplementary Figure 24 The schematic model for the twisting. This figure shows the corresponding {111} planes of metal core and c-ZrO_2 connect with each other. This twisting minimizes the energy of semi-coherent interfaces. The metal Zr atoms and oxide Zr atoms are colored in deep red and ivory, respectively.

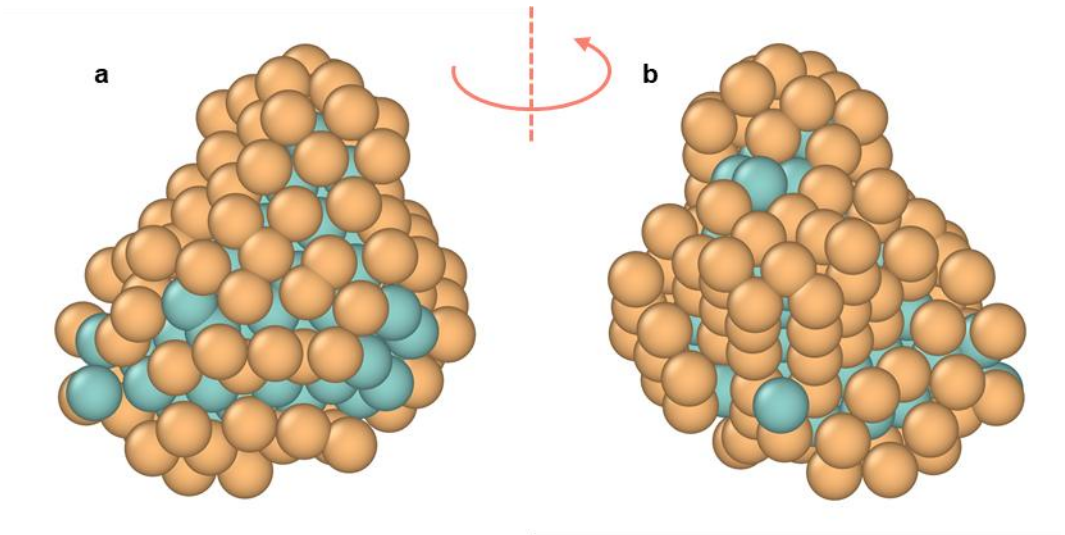

Supplementary Figure 25 All {111} faces are colored in orange in metal core, while the other atoms are colored in green. a, In the direction of one {111} face. **b**, Rotate the metal core to the back.

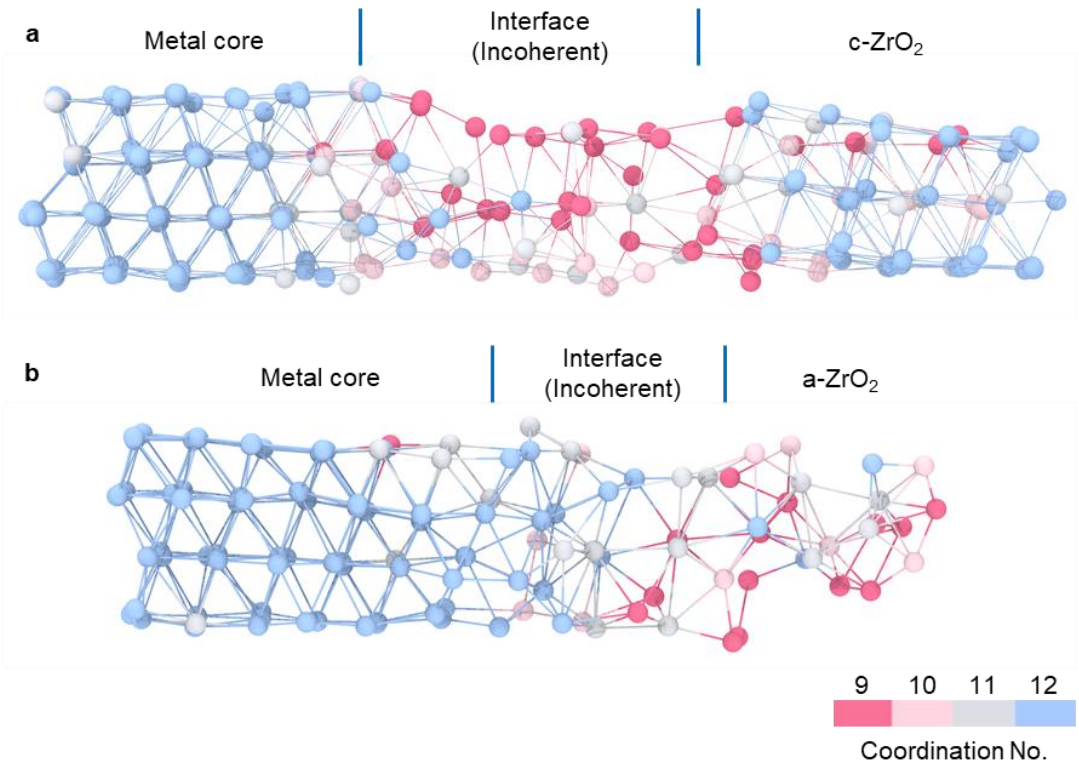

Supplementary Figure 26 Coordination number. Coordination number of metal/c-ZrO_2 (**a**) and metal/a-ZrO_2 (**b**) incoherent interface. The coordination number is lower at the incoherent interface.

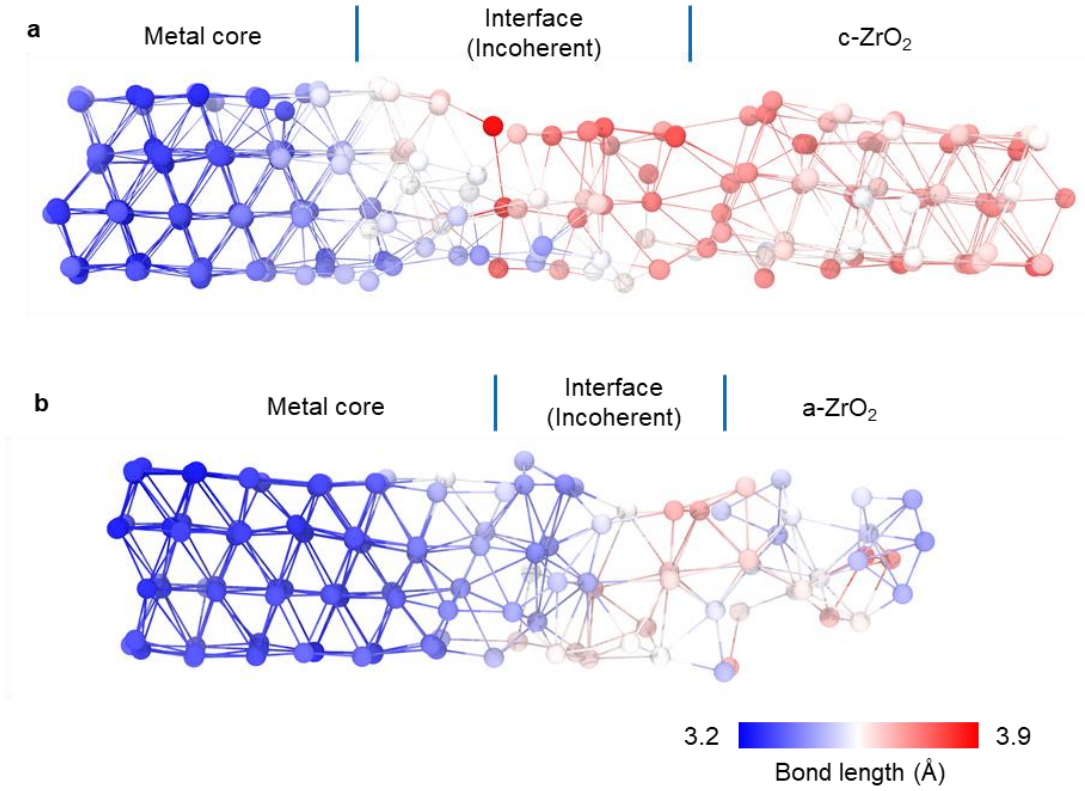

Supplementary Figure 27 Averaged bond length. Averaged bond length (in Å) of metal/c-ZrO_2 (**a**) and metal/a-ZrO_2 (**b**) incoherent interface. The bonds are longer at the incoherent interface.

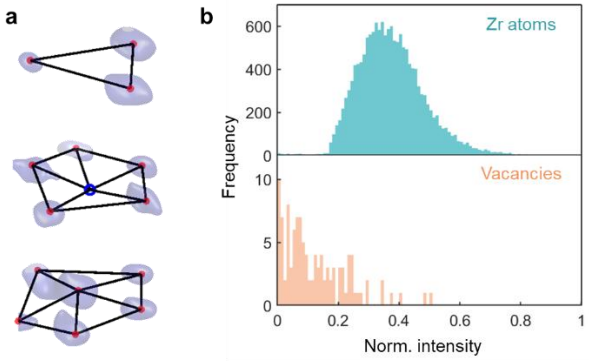

Supplementary Figure 28 3D determination of a vacancy in the Zr1 nanoparticle. a, 3D surface renderings of one representative vacancy in Zr1. The blue isosurface shows the intensity distribution of volume around the vacancy. The red dots are the positions of Zr atoms around the vacancy. The blue circle highlights the position of the Zr vacancy. **b**, The intensity histogram for all the Zr atoms (up panel) and all the vacancies (down panel) in Zr1. The intensity of vacancies is much lower than those of the Zr atoms.

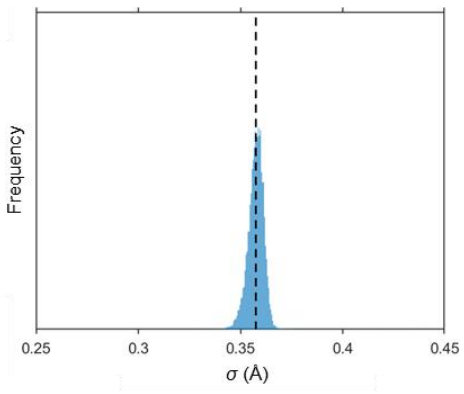

Supplementary Figure 29 The distribution of parameter *σ*. The mean value of σ (0.357 Å) is marked by the dashed line.

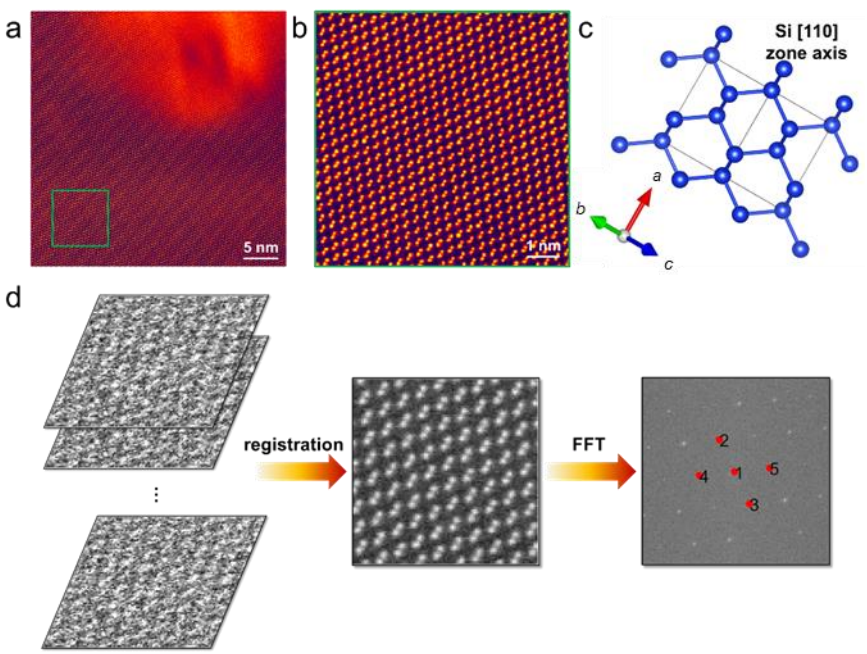

Supplementary Figure 30 Calibration of the pixel size for the ADF-STEM images. a, ADF-STEM image of Si [110] zone axis. **b**, Magnified image of the green box in **a**. **c**, Crystal structure of cubic structured Si projected along [110] zone axis. **d**, Image processing procedure including registration and fast Fourier transform. The lattice spacing is measured based on the distance of point 2-5 to the central point 1.